Ratiometric fluorescent chemosensor for mercury(II) cations in aqueous solution based on the crown-containing bis(chromophoric) 1,8-naphthalimide—styrylpyridine system*

P. A. Panchenko,[a,b★] A. S. Polyakova,[a] M. A. Ustimova,[a] A. V. Efremenko,[c] A. V. Feofanov,[c,d] Yu. V. Fedorov,[a] and O. A. Fedorova[a,b]

[a]*A. N. Nesmeyanov Institute of Organoelement Compounds, Russian Academy of Sciences, Build. 1, 28 ul. Vavilova, 119334 Moscow, Russian Federation. E-mail: pavel@ineos.ac.ru*

[b]*D. I. Mendeleev University of Chemical Technology of Russia, 9 Miusskaya pl., 125047 Moscow, Russian Federation*

[c]*M. M. Shemyakin—Yu. A. Ovchinnikov Institute of Bioorganic Chemistry, Russian Academy of Sciences, 16/10 ul. Miklukho-Maklaya, 117997 Moscow, Russian Federation*

[d]*Department of Biology, M. V. Lomonosov Moscow State University, Build. 12, 1 Leninskie Gory, 119234 Moscow, Russian Federation*

The crown-containing bis(chromophoric) chemosensor for mercury(II) cations in an aqueous solution was synthesized using the azide—alkyne 1,3-dipolar cycloaddition click reaction. The synthesized compound contains the 4-methoxy-1,8-naphthalimide fragment acting as the electron excitation energy donor and styrylpyridine being the chromorphore-acceptor. Upon the excitation of the naphthalimide residue with the visible light, the resonance energy transfer (RET) occurs, and its efficiency decreases as a result of complex formation with Hg^{2+} cations. The changes in the fluorescence spectrum observed upon the addition of Hg^{2+} allow one to detect the ratiometric fluorescence response due to an increase in the ratio of emission intensities in the donor and acceptor channels. Based on the spectrophotometric and spectrofluorimetric titration data, the logarithms of the stability constants ($\log K$) for the 1 : 1 metal—ligand complex were calculated to be 5.37±0.05 and 5.81±0.06, respectively. The proposed fluoroionophore is characterized by the detection limit of Hg^{2+} ions in water at pH 4.5 equal to 40 nmol L^{-1}. The ability of the synthesized chemosensor to perform fluorescence imaging of mercury(II) cations in living cells was also analyzed.

Key words: sensor, fluorescence imaging, 1,8-naphthalimide, styryl dye, mercury(II) cation, resonance energy transfer, intramolecular charge transfer, HEK 293 cells, Heck reaction, azide—alkyne 1,3-dipolar cycloaddition.

The development of fluorescent chemosensors for the detection of heavy and transition metal cation is presently a topical trend in the chemistry of photoactive organic compounds.[1—6] In this respect, the mercury(II) cation is one of the most significant analytes. Mercury is widely abundant in the environment because of human activity. The Hg^{II} ions are easily transformed by sea microorganisms into methylmercury ($MeHg^+$), which is more harmful than inorganic or elemental mercury.[7,8] Further heaving *via* the food cycle, $MeHg^+$ can be accumulated in fish organisms.[9] This is dangerous for human health. The extremely high toxicity of the mercury compounds is caused by high affinity to thiol groups of proteins and enzymes,[10] which induces cell disfunction and, as a consequence, results in damages of the digestive, cardiovascular, and central nervous systems.[11,12] Many sensors for this cation are described in the modern literature, and this information was systematized in the recent reviews.[13—15]

The most important requirements imposed in sensor devices for the detection of metal cations

* On the occasion of the 70th anniversary of the foundation of A. N. Nesmeyanov Institute of Organoelement Compounds of the Russian Academy of Sciences.

Published in Russian in *Izvestiya Akademii Nauk. Seriya Khimicheskaya,* Vol. 73, No. 10, pp. 2921—2935, October, 2024.

under *in vitro* and *in vivo* conditions are possibilities of working in a highly competitive aqueous medium and exhibiting the ratiometric fluorescence response to the presence of the analyte. According to the ratiometric procedure of measurements, the fluorescence intensity can be measured at different excitation or emission wavelengths, and the ratio of these intensities would change depending on the content of the determined substance.[16—19] In this case, it is not necessary to know the concentration of fluoroionophore molecules in the system under study to calculate the equilibrium concentration of the determined substance. Note that the widely abundant fluorescent PET chemosensors,[20] which function on the basis of the mechanism of photoinduced electron transfer (PET) and are built according to the fluorophore—spacer—receptor type, demonstrate fluorescence enhancement or quenching upon the reaction with the analyzed substrate without changing the shape and position of the emission band maximum. This does not allow one to perform analysis in a biological medium, for instance, in living cells.

The simplest method to achieve a ratiometric response is the introduction into the molecule of the ICT fluorophore (compound, whose absorption and fluorescence in the long-wavelength spectral range are associated with the intramolecular charge transfer (ICT)) of the receptor group in such a way that one or several electron-donor atoms of the receptor are included into the chromophoric system of the dye. The compounds exhibiting the properties of ICT chemosensors are formed in this case. Their characteristic feature of the shift is maxima in the absorption and emission spectra upon complex formation due to a change in the energy of the ICT transition.[21] The examples of the monochromophoric ratiometric ICT chemosensors for the mercury(II) cations were described.[22—25] However, their practical use is accompanied by two problems. The first problem is the fluorescence quenching of the photoactive fragment due to the contact of its π-system with the Hg^{2+} cation in the complex (so-called internal heavy atom effect).[26] As known, the use of fluorescence quenching as an analytical signal is less preferable than the enhancement of fluorescence since leads to an increase in the relative error of analysis.[27,28] The second problem is that for the monochromophoric ICT chemosensors the shift of the fluorescence band maximum (λ^{fl}_{max}) is often observed in a range of 20—50 nm,[29—32] which results in an insignificant change in the ratio of fluorescence intensities at two different wavelengths, *i.e.*, in a weakly pronounced ratiometric response. One of possible causes for this type behavior can be the recoordination of the metal cation in the receptor cavity leading to the cleavage of the bond between the cation and fluorophore[32] due to which the optical characteristics of the latter in the complex are close, to a significant extent, to its characteristics in the free ligand.

The use of the resonance energy transfer (RET) of electron excitation between the chromorphore-donor (CD) and chromophore-acceptor (CA) is a very successful strategy to achieve the ratiometric fluorescence response.[33—35] In the case of the bis(chromophoric) RET chemosensors, the interaction with the substrate induces a change in the efficiency of the resonance energy transfer (Φ_{RET}) in the system, which, in turn, leads to a change in the ratio of intensities of the emission peaks of CD and CA in the spectrum. Several ratiometric RET chemosensors for the mercury(II) cations have been described to date. The principle of the operation of the majority of them is based on using the cation-induced opening of the spirolactam cycle of the rhodamine dyes, which act as excitation energy acceptors in these compounds.[36—40]

In our recent work,[41] we showed a possibility of switching over the RET process in the bis(chromophoric) system based on the naphthalimide-containing PET sensor for the Hg^{2+} cation acting as CD and styryl dye (CA) due to a change in the competition between RET and PET upon complex formation. In the present study, we propose the method for increasing the ratiometric response of the ICT chemosensor due to using the resonance energy transfer. Styrylpyridinium dye **1** was chosen as the ICT fluoroionophore, since its unshared electron pair of the nitrogen atom of the crown ether receptor is conjugated with the electron-acceptor pyridine fragment. The sensor properties of compound **1** were studied by us earlier.[42] The studies showed that chemosensor **1** in an aqueous solution at pH 6.0 formed with the mercury(II) cations the stable complex **1** · Hg^{2+}, which is characterized by the logarithm of the stability constant (log$K$) equal to 6.03±0.06. The binding of the cations is accompanied

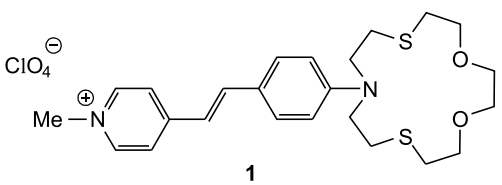

1

Scheme 1

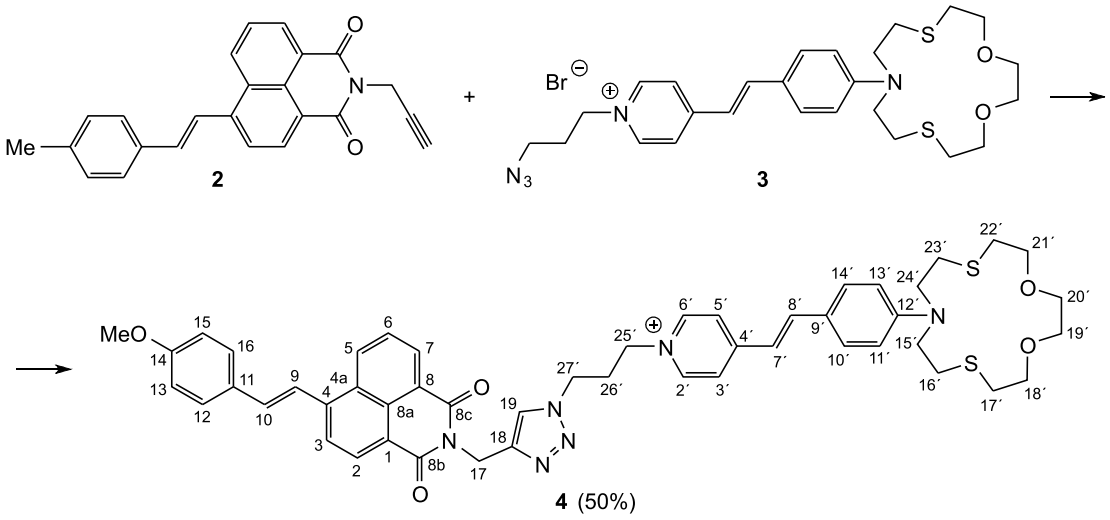

Reagents and conditions: CuI, diisopropylethylamine (DIPEA), DMF, Δ.

by the hypsofluoric and hyperfluoric effects. Nevertheless, the hypsofluoric shift on going from ligand **1** to complex **1** · Hg^{2+} turned out to be low (36 nm).

In order to improve the sensor properties of ICT chemosensor **1**, we modified its structure (Scheme 1) by the introduction of the 4-styryl-1,8-naphthalimide chromophoric fragment with the formation of RET pair **4**.

The 1,8-naphthalimide derivatives are among the most popular classes of organic luminophores, which is widely used in the development of optical molecular devices of different design,[43—46] including fluorescent chemosensors.[47—53] The results of studying the sensor properties of compound **4** with respect to mercury(II) cations in an aqueous solution and in living cells are presented below.

Results and Discussion

The Cu^{I}-catalyzed click reaction of 1,3-dipolar azide—alkyne cycloaddition (see Scheme 1) was used for the preparation of RET system **4**. Derivative **3**, which was formed (Scheme 2) upon the condensation of aldehyde **6** with the earlier[41] synthesized γ-picolinium salt **5**, served as "azide." The second component of the click reaction ("alkyne") was the derivative of 4-styryl-1,8-naphthalimide **2** with the propargyl group, easily available *via* the Heck reaction between styrene **7** and 4-bromonaphthalic anhydride **8** followed by the imidation of anhydride **9** with propargylamide (Scheme 3). Aldehyde **6** was synthesized *via* the previously described[54] procedure.

The spectral and complexation properties of bis(chromophoric) derivative **4** and model compounds **1** and **2** (being individual monochromophoric components of RET pair **4**) were studied in an aqueous acetate buffer at pH 4.5. On the one hand, at the indicated pH the azadithia-15-crown-5-ether fragment in compounds **1** and **4** efficiently binds the mercury(II) ions[55] (in the neutral medium the complex formation is suppressed because of the hydrolysis of mercury(II) perchlorate[56] used in the work). On the other hand, no protonation of the nitrogen

Scheme 2

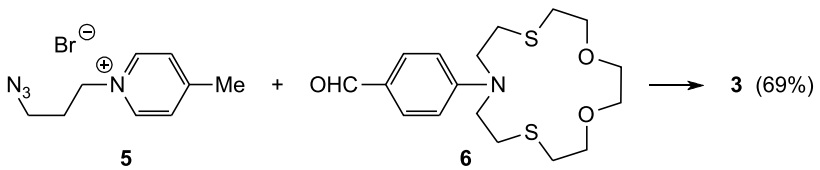

Reagents and conditions: piperidine, EtOH, Δ.

Scheme 3

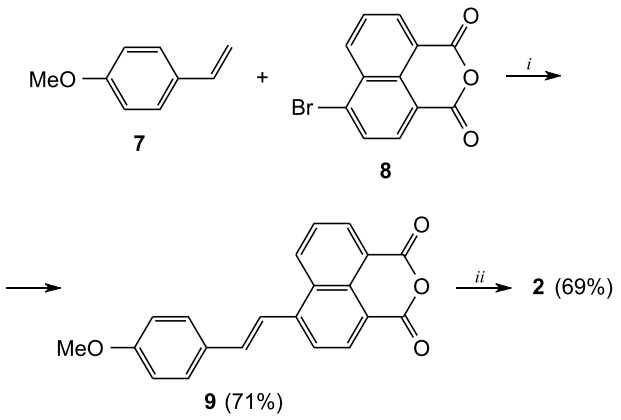

Reagents and conditions: *i*) $Pd(OAc)_2$, P(*o*-Tol)$_3$, NEt_3, DMF, Δ; *ii*) propargylamine, 2-methoxyethanol, Δ.

atom of the receptor is observed.[42,55] The optical response of styryl dye **1** to the presence of Hg^{2+} under the described conditions was first analyzed.

Binding of mercury(II) cations with compound **1** was accompanied by the appearance in the absorption spectrum of the band at 350 nm corresponding to the 1 : 1 metal—ligand complex (Fig. 1, *a*; Table 1). The intensity of the long-wavelength band with a maximum at 457 nm, which is associated with the intramolecular charge transfer in the free ligands, decreases. In the fluorescence spectrum of compound **1**, complex formation induces the shift of the band maximum to the short-wavelength range and an increase in its intensity (Fig. 1, *b*). These spectral changes are the result of increasing the energy of the ICT transition in the complex due to a decrease in the electron-donor properties of the nitrogen atom of the macrocyclic receptor. The stability constant of complex **1** · Hg^{2+} was determined from the data of spectrophotometric and spectrofluorimetric titration of compound **1** with mercury(II) perchlorate (see Table 1) (for the procedure of determination of the stoichiometry of the complex, see Experimental). The determined values turned out to be higher than the earlier calculated stability constant of complex **1** · Hg^{2+} in water ($\log K = 6.03 \pm 0.06$),[42] which is likely related to the difference in the pH at which the complex formation was studied (pH 6.0 in Ref. 42 and 4.5 in this work).

The choice of the 4-methoxystyryl-1,8-naphthalimide as CD in the structure of RET pair **4** is based on an analysis of the spectral characteristics of individual dyes **1** and **2**. So, the absorption spectrum of compound **1** (CA) is overlapped with the emission spectrum of derivative **2** (Fig. 2). This overlap provides a possibility of RET to occur in free ligand **4**. At the same time, the hypsochromic shift of the absorption maximum of CA upon complex formation with Hg^{2+} (see Fig. 1) induces a decrease in the overlapping the spectral bands and a decrease in the RET efficiency, which should be observed as an increase in the intensity of the emission band of CD in the spectrum against the background of the signal of CA (Scheme 4). The overlapping inte-

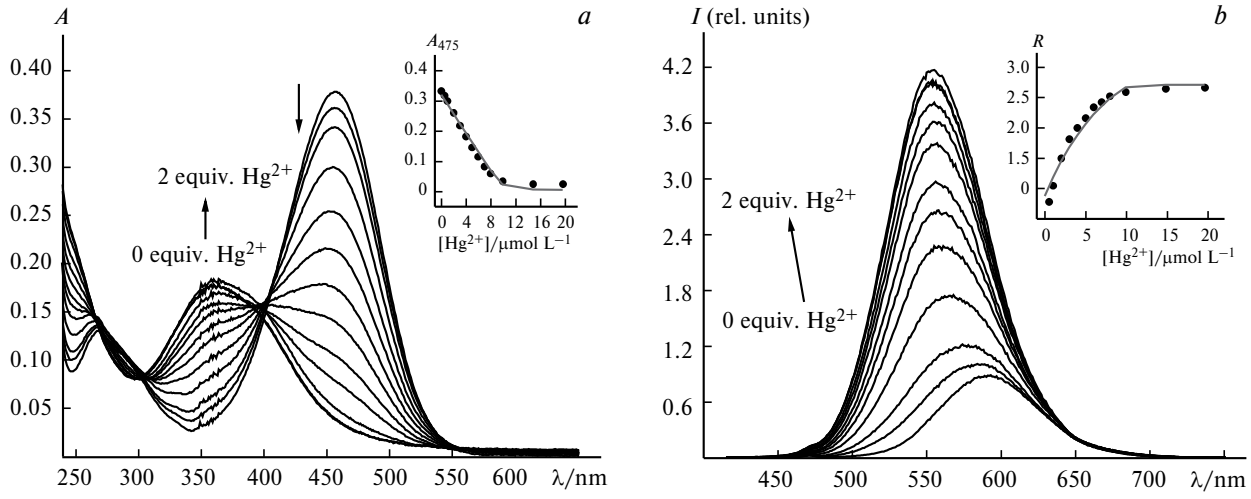

Fig. 1. Changes in the absorption (*a*) and fluorescence (*b*) spectra of compound **1** (10.0 μmol L^{-1}) upon the gradual addition of mercury(II) perchlorate in water at pH 4.5 (acetate buffer, 0.01 mol L^{-1}). The excitation wavelength is 405 nm. Insets: absorbance at 475 nm (A_{475}) and ratio *R* of the fluorescence intensities at 550 and 605 nm (I_{550}/I_{605}) *vs* concentration of $Hg(ClO_4)_2$ in a solution (points are experimental data, and curves are calculation).

Table 1. Spectral characteristics of compounds **1**, **2**, and **4** and stability constants of complexes **1** and **4** with mercury(II) cations in water at pH 4.5[a]

Compound (L)	λ^{abs}_{max}	λ^{fl}_{max}	φ^{fl}	$\log K^b$ for $L \cdot Hg^{2+}$	
	nm			spectrophotometry data	spectrofluorimetry data
2	425	595	0.039	—	—
1	460	610	0.0066	7.4±0.4	7.6±0.6
4	469	637	0.00085	5.37±0.05	5.81±0.06

[a] Acetate buffer, 0.01 mol L^{-1}.
[b] The dimensionality of constant K is L mol^{-1}.

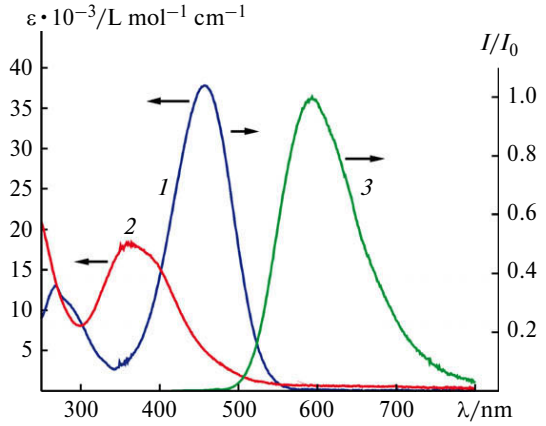

Fig. 2. Overlapping of the absorption spectra of compound **1** (*1*) and complex **2** · Hg^{2+} (*2*) with the normalized fluorescence spectrum of compound **2** (*3*) in water at pH 4.5 (acetate buffer, 0.01 mol L^{-1}). The excitation wavelength is 415 nm. The concentration of all compound in the solution is 10.0 μmol L^{-1}.

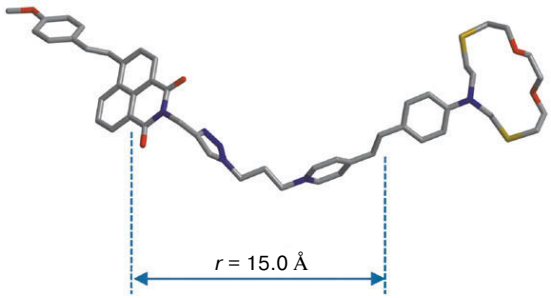

Fig. 3. Geometry of compound **4** optimized by the PM6 method.

grals $J(\lambda)$, Förster critical radii R_0, and efficiencies resonance energy transfer Φ_{RET} for the pairs of chromophores **1**—**2** and **1** · Hg^{2+}—**2** determined in terms of the inductive resonance model of RET,[57] are given in Table 2 for clarity. The data on the optimized geometry of compound **4** (Fig. 3) and the spectral characteristics of the individual chromophores were used for the calculation of these parameters. The details of the calculation are given in Experimental.

The absorption spectrum of chemosensor **4** contains a broad long-wavelength band bathochromically shifted relatively to the band of styryl dye **1** (Fig. 4, *a*). The shift by 27 nm to the red range on going from compound **1** to **4** was also observed in the fluores-

Table 2. Spectroscopic characteristics of the RET pairs naphthalimide—styryl dye in water

RET pair	$J(\lambda)$ /nm^4 L mol^{-1} cm^{-1}	R_0/Å	Φ_{RET}
2 (CD)—**1** (CA)	$1.65 \cdot 10^{14}$	20.7	0.89
2 (CD)—**1** · Hg^{2+} (CA)	$8.87 \cdot 10^{13}$	12.7	0.30

Scheme 4

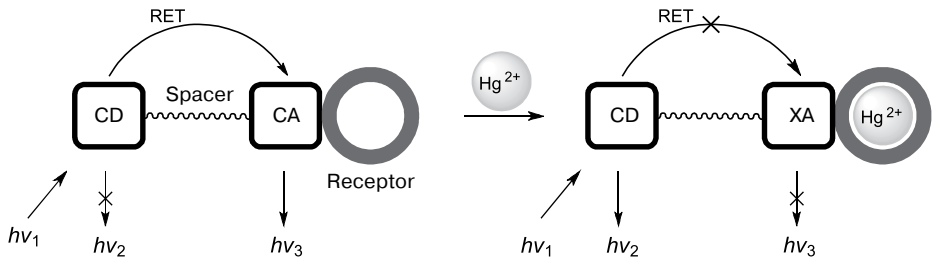

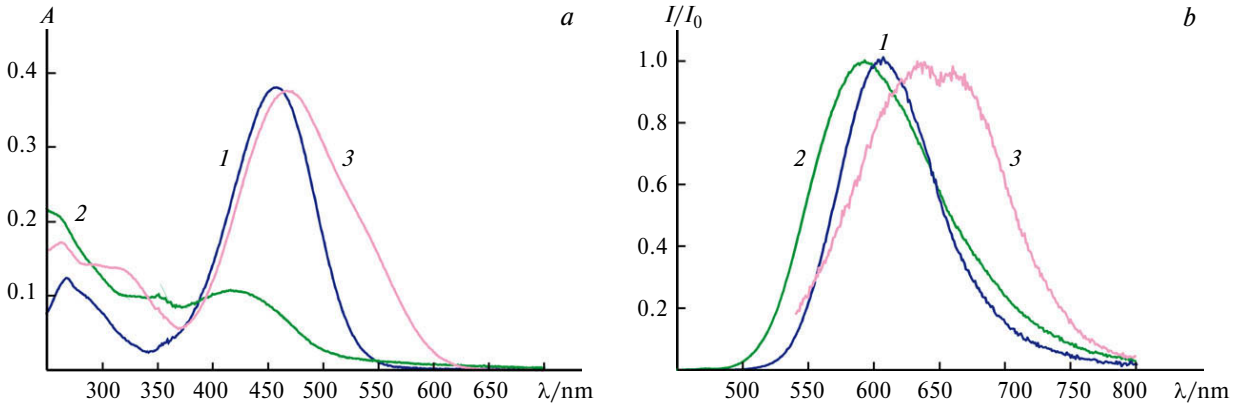

Fig. 4. Absorption spectra (*a*) and normalized fluorescence spectra (*b*) of compounds **1** (*1*), **2** (*2*), and **4** (*3*) in water at pH 4.5 (acetate buffer, 0.01 mol L^{-1}). The concentration of all compound is 10.0 μmol L^{-1}. The excitation wavelength is 405 (**2**, **4**) and 460 nm (**1**).

cence spectrum (Fig. 4, *b*; see Table 1). The mentioned bathochromic shift is not related to the contribution of the absorption band of the chromophore-donor, because the latter lies in a shorter-wavelength range (in the absorption spectrum of naphthalimide **2** this band represents a maximum at 420 nm, see Fig. 4, *a*). It is most likely that some change in the degree of polarization of the π-electron system of the styrylpyridinium chromophore is observed due to the addition of the second photoactive fragment, since this chromophore is highly sensitive to the microenvironment.

The above mentioned assumption is confirmed by the fact that the chemical shifts of protons of the naphthalimide core in compounds **2** and **4** are nearly indiscernible in the ^{1}H NMR spectra, whereas the signals of the styrylpyridinium fragment undergo a significant shift on going from compound **3** to **4** (Table 3), and also by the fact that the stabilities of complexes **1** and **4** with the mercury(II) cation differ by approximately two orders of magnitude (see Table 1).

The addition of Hg^{2+} to an aqueous solution of compound **4** (acetate buffer, pH 4.5) resulted in the hypsochromic shift of the long-wavelength absorption band caused by the coordination of the cation with the crown ether fragment of the styrylpyridinium residue (Fig. 5, *a*). The presence of Hg^{2+} resulted in the shift of the maximum in the fluorescence spectrum of compound **4** to the short-wavelength range and an increase in the emission intensity (Fig. 5, *b*). Taking into account the data presented, the logarithm of the stability constant of the 1 : 1 complex of com-

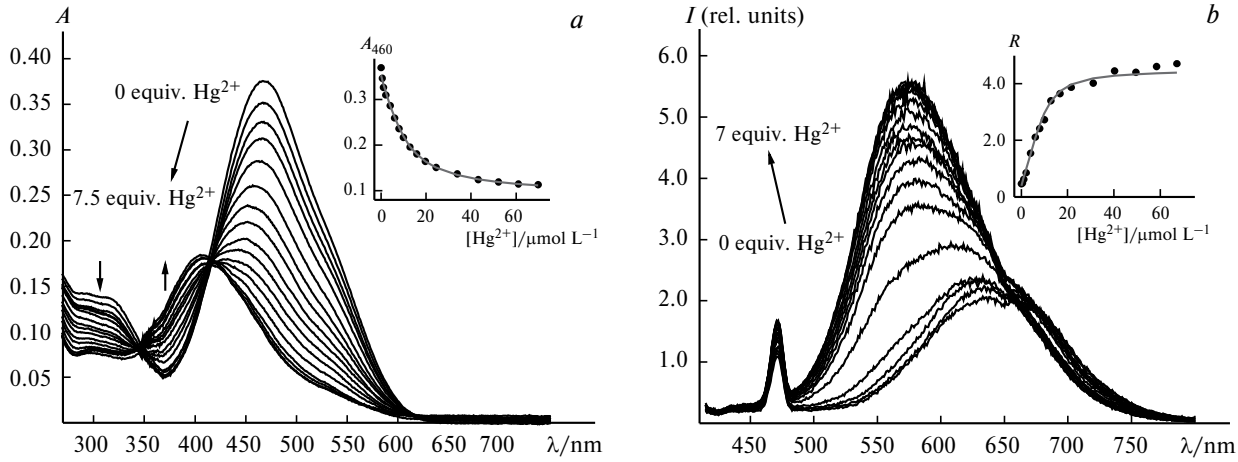

Fig. 5. Changes in the absorption (*a*) and fluorescence (*b*) spectra of compound **4** (10.0 μmol L^{-1}) upon the gradual addition of mercury(II) perchlorate in water at pH 4.5 (acetate buffer, 0.01 mol L^{-1}). The excitation wavelength is 405 nm. Insets: absorbance at 460 nm (A_{460}) and ratio R of the fluorescence intensities at 565 and 687 nm (I_{565}/I_{687}) *vs* concentration of $Hg(ClO_4)_2$ in a solution (points are experimental data, and curves are calculation). The peak at 470 nm corresponds to the Raman signal of the solvent.

Table 3. Chemical shifts of protons in the ^1H NMR spectra of compounds **2**—**4** in DMSO-d_6

Hydrogen atom[a]	δ		$\lvert\delta_1 - \delta_2\rvert$[b]
	Monochromophore, compound **2** or **3** (δ_1)	Bis(chromophore), compound **4** (δ_2)	
	Naphthalimide fragment		
OCH_3	3.82	3.82	0
H(17)	4.79	5.30	**0.51**
H(13), H(15)	7.02	7.03	0.01
H(10)	7.59	7.60	0.01
H(12), H(16)	7.83	7.83	0
H(6)	7.88—7.95	7.88—7.95	**0.06**
H(9)	8.08	8.09	0.01
H(3)	8.23	8.24	0.01
H(2)	8.49	8.50	0.01
H(7)	8.57	8.56	0.01
H(5)	9.03	9.04	0.01
	Styrylpyridinium fragment		
H(26′)	2.10—2.22	1.13—1.25	**0.97**
H(16′), H(23′)	2.71—2.79	2.72—2.78	0.01
H(17′), H(22′)	2.80—2.89	2.79—2.87	0.01
H(27′)	3.43—3.51	3.44—3.50	0.01
H(15′), H(24′)	3.53—3.62	3.55—3.60	0.02
H(18′), H(19′), H(20′), H(21′)	3.62—3.75	3.63—3.73	0.01
H(25′)	4.43—4.54	4.37—4.47	**0.06**
H(11′), H(13′)	6.72	6.71	0.01
H(8′)	7.17	7.11	**0.06**
H(10′), H(14′)	7.59	7.53—7.64	**0.06**
H(7′)	7.94	7.86—7.96	**0.08**
H(3′), H(5′)	8.08	8.01	**0.07**
H(2′), H(6′)	8.78	8.69	**0.09**

[a] The numeration of atoms in the naphthalimide and styrylpyridinium fragments of compounds **2**—**4** is shown in Scheme 1.

[b] The differences in chemical shifts corresponding to the protons, whose signals most strongly change their positions in the spectrum on going from the monochromophoric derivative (**2** or **3**) to bis(chromophore) **4**, are emphasized by bold.

pound **4** with the Hg^{2+} cation was estimated (see Table 1). The observed enhancement of fluorescence of compound **4** is a partial result of increasing the radiative deactivation efficiency of the styrylpyridinium chromophore itself upon complex formation (see Fig. 1, *b*) and a result in part of an increase in the emission intensity of CD due to the suppression of RET (emission bands of compounds **2** and **1** · Hg^{2+} are strongly overlapped, see Fig. 4, *b* and Fig. 1, *b*). The change in the shape of the fluorescence spectrum of complex **4** upon Hg^{2+} binding makes it possible to consider this sensor as ratiometric. In fact, the R ratio of fluorescence intensities at 565 and 687 nm ($R = I_{565}/I_{687}$) increases by approximately 9 times during spectrofluorimetric titration (see inset in Fig. 5, *b*). Note that, under similar conditions, monochromophoric ratiometric chemosensor **1** demonstrated a lower contrast in switching over the analytic signal (ratio R, which was equal to I_{550}/I_{605}, increased by 3.5 times upon the addition of mercury(II) perchlorate, see Fig. 1, *b*).

The spectral response of sensor **4** to the Hg^{2+} ion was selective: no changes were observed in the absorption and fluorescence spectra in the presence of Zn^{2+}, Cd^{2+}, Cu^{2+}, Ag^{+}, Ni^{2+}, Pb^{2+}, Ca^{2+}, Mg^{2+}, and Fe^{2+} cations. The histogram presented in Fig. 6 shows the increase in I_{565}/I_{687} upon the addition of 5 equivalents of perchlorate of the

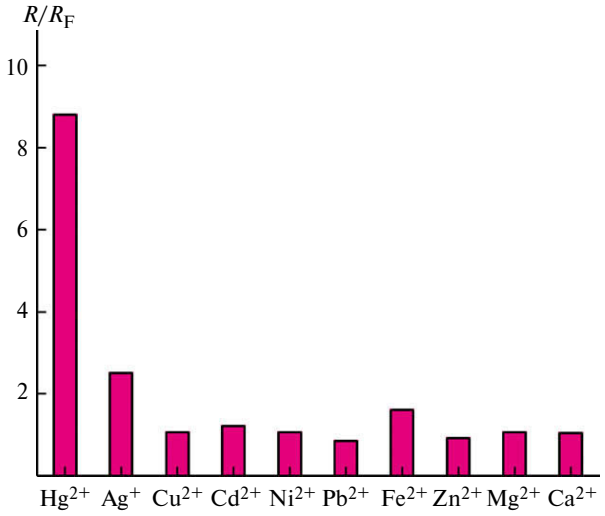

Fig. 6. Fluorescence response of sensor **4** (10.0 μmol L^{-1}) to the presence of metal cations in an aqueous solution at pH 4.5 (acetate buffer, 0.01 mol L^{-1}). The R_F value is calculated as the ratio of the fluorescence intensities at 565 and 687 nm for free ligand **4**, and R is the analogous ratio after the addition of metal perchlorate (5 equiv.) to a solution of sensor **4**. The excitation wavelength is 405 nm.

indicated metals to an aqueous solution of compound **4**.

The dependence of the R ratio on the fluorescence intensities at wavelengths of 565 and 687 nm for sensor **4** exhibits a good linear correlation (correlation coefficient 0.97) with the Hg^{2+} concentration in a range of 1—10 μmol L^{-1} (Fig. 7). Taking into

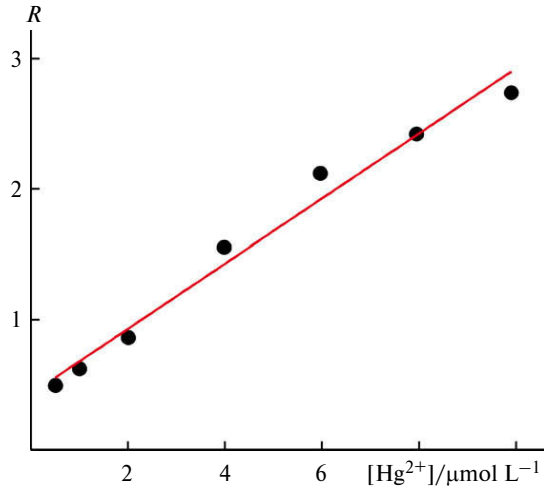

Fig. 7. Ratio (R) of the fluorescence intensities at 565 and 687 nm (I_{565}/I_{687}) of a solution of compound **4** (10.0 μmol L^{-1}) in water at pH 4.5 (acetate buffer, 0.01 mol L^{-1}) *vs* concentration of $Hg(ClO_4)_2$ in a solution (points are experimental data, and curves are the linear approximation by least squares). The excitation wavelength is 405 nm.

account the slope ratio r of the presented calibration straight line (see Fig. 7) and the standard deviation of the analytical signal s (R ratios), we found by Eq. (1)[58] that the detection limit (C_{DL}) of Hg^{2+} cations using sensor **4** under specified conditions was 40 nmol L^{-1}. The determined value of C_{DL} turned out to be close to the maximum permissible concentration of mercury in the drinking water (30 nmol L^{-1}).[59]

$$C_{DL} = 3s/r \quad (1)$$

Finally, we analyzed a possibility of using sensor **4** for fluorescent imaging of mercury(II) cations in the living cells. The HEK293 embryonal cells from the human kidney were used for the study. As compound **4** is added to the cells from the stock solution in DMSO, its significant portion in the cellular medium precipitates, which is likely related to a high hydrophobicity of the compound. It was found by laser scanning confocal microscopy (LSCM) that compound **4** penetrated into the HEK293 cells and was accumulated in the cytoplasm. In this case, the compound was concentrated in vesicles and localized in the elongated cellular organoids, and the diffusion coloration of the cytoplasm was observed (Fig. 8, *a*, *b*). The character of the intracellular distribution of the compound does not substantially change upon the variation of the incubation concentrations and incubation duration of the cells. The obtained intracellular fluorescence spectra of the compound localized in the submicron vesicular structures differ in shape and position of the maximum (λ^{fl}_{max} 572 nm) from the spectra in other parts of the cytoplasm (λ^{fl}_{max} 577 nm) (Fig. 8, *c*, *d*). The intensity of the intracellular fluorescence spectra varies in different parts of the cell.

To reveal the origin of vesicles that accumulate compound **4**, we performed the colocalization analysis of the compounds under study with the Lyso Tracker Red (LR) fluorescent marker of lysosomes. It is elucidated by the LSCM method that the granular distribution of the compound observed in the cells reflects its predominant accumulation in lysosomes (Fig. 9). The colocalization coefficient of the compound with lysosomes is 0.7±0.1. Note that monochromophoric styryl dye **1** penetrated into living cells and was accumulated predominantly in mytochondria.[42] As shown by the previous results,[42] it was impossible to detect Hg^{2+} in the cells using compound **1** because of the basic level of pH (about 8.0) in the indicated organellas. When study-

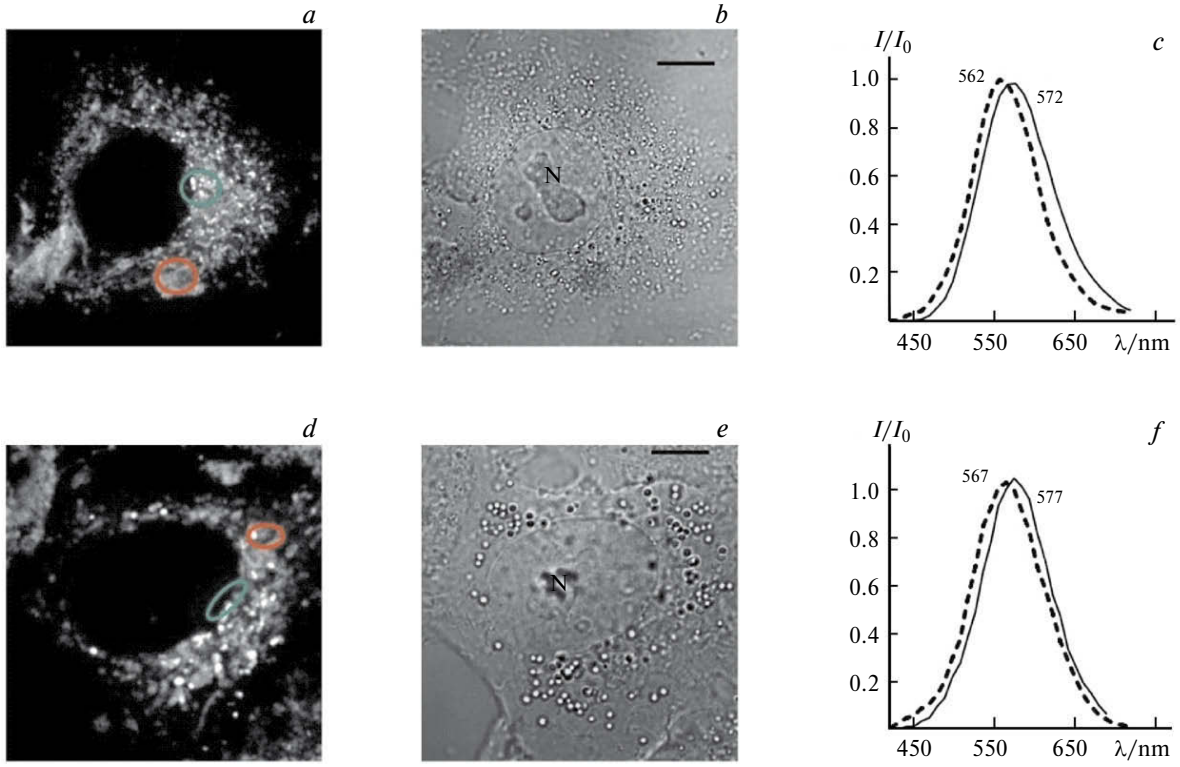

Fig. 8. Confocal fluorescent images (*a*, *b*, *d*, *e*) and intracellular fluorescence spectra of compound **4** (*c*, *f*, solid lines) and complexes **4**·Hg^{2+} (*c*, *f*, dashed lines) in the vesicular structures (*c*) and cytoplasm (*f*) in the HEK293 cells; *a*, *d* are fluorescent images; *b*, *c* are images of the cells in transmitted light. The cells were incubated with compound **4** (5 μmol L^{-1}) for 1 h (*a*, *b*) or pre-incubated with $Hg(ClO_4)_2$ (50 μmol L^{-1}) for 30 min and then incubated with compound **4** (5 μmol L^{-1}) for 1 h (*d*, *e*). The scale mark is 5 μm. The fluorescence excitation wavelength is 405 nm, and fluorescence was detected in a range of 420—730 nm. The fluorescence spectra were normalized relatively to the intensity of the signal at the maximum point (I_0). Green ovals show some lysosomes, and red ovals show the region of diffuse distribution of the compound in the cytoplasm or an organoid different from a vesicle. Letter "N" indicates nuclei.

ing the intracellular complex formation of sensor **4**, we started from the assumption that the binding of Hg^{2+} cations by the azadithiacrown-ether receptor was not suppressed by the hydrolysis of the mercury salt, since the pH in lysosomes is approximately 4.5.[60] The complex formation of the fluorescent sensors based on azadithia-15-crown-5-ether with Hg^{2+} in the lysosomes was described previously.[41,42]

The pre-incubation of the HEK293 cells with $Hg(ClO_4)_2$ (20—50 μmol L^{-1}, 60 min) and further incubation with complex **4** (5 μmol L^{-1}, 60 min) resulted in the shift of the intracellular fluorescence spectra to the short-wavelength range by 10 nm (see

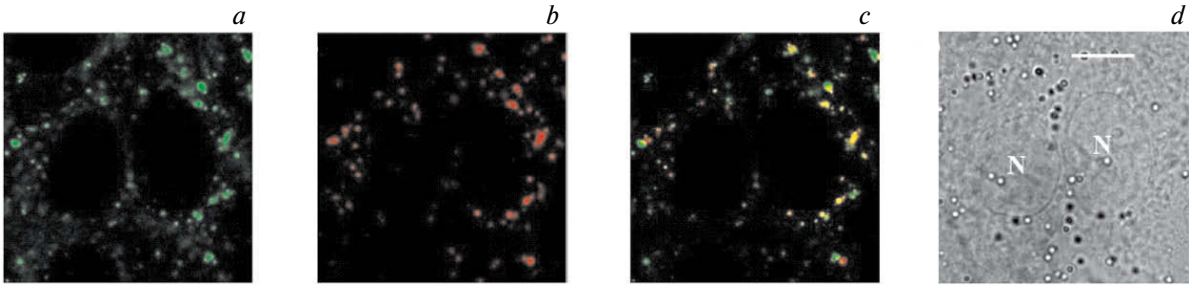

Fig. 9. Typical distributions of compound **4** (*a*) and fluorescent marker of lysosomes LR (*b*) in the HEK293 cells obtained by the LSCM method; (*c*) superposition of the images (*a*) and (*b*). Yellow color indicates the colocalization of compound **4** and LR marker. The fluorescent images were corrected to the overlapping of the spectra of the fluorophores; (*d*) image of the cells in transmitted light. The scale mark corresponds to 10 μm. Letter "N" indicates nuclei.

Fig. 8). An analogous result was observed for the incubation of the cells with compound **4** and subsequent incubation with $Hg(ClO_4)_2$. The maximum of the intracellular fluorescence spectrum of compound **4** in the presence of Hg^{2+} was detected at 562 and 567 nm in the lysosomes and cytoplasm, respectively (see Fig. 8, *c*, *d*). The insignificant change in the emission band shape and a slight shift of the maximum in the presence of Hg^{2+} ions in the cells are probably related to the fact that the fluorescence spectrum of the styryl dye acting as CA in chemosensor **4** shifts to the short-wavelength range on going from an aqueous solution to the intracellular medium (similarly to that described previously[41,42] for similar styryl derivatives). As a result, the difference in the positions of the emission maxima of CA, CD, and CA bound to the Hg^{2+} ion is insufficient for the detection of the ratiometric fluorescence response. Thus, we synthesized bis(chromophoric) chemosensor **4** exhibiting the selective ratiometric fluorescent response to the presence of mercury(II) cations in an aqueous solution. As compared to monochromophoric ICT chemosensor **1**, the synthesized compound demonstrated a high contrast in changing the analytical signal (ratio of the fluorescence intensities at two different wavelengths), which is caused by the enhancement of fluorescence of the chromophore-donor due to a change in the energy transfer efficiency in the system. It is found that the introduction of the naphthalimide chromophore fragment into styryl dye **1** induces a change in the character of the intracellular distribution and provides the accumulation of sensor reagent **4** in the lysosomes and in the cytoplasm, where the binding of Hg^{2+} ions is also possible. The intracellular emission spectra of free and Hg^{2+}-bound chemosensor **4** differ in the position of the maximum; *i.e.*, chemosensor **4** reacts to the presence of Hg^{2+} in the living cells. Nevertheless, the hypsofluoric shift of the emission maximum of the styrylpyridinium residue, which occurs on going from an aqueous solution to the intracellular medium, worsens the ratiometric response. The presented data on studying the cation-dependent spectral properties of compound **4** in an aqueous solution show advantages of using the RET process for the development of ratiometric fluorescent chemosensors.

Experimental

^1H and ^{13}C NMR spectra were recorded on an Avance 400 spectrometer (Bruker; ^1H, 400.13 MHz; ^{13}C, 100.60 MHz). Chemical shifts for ^1H and ^{13}C were determined with an accuracy of 0.01 ppm relative to the residual signals of the solvent and recalculated to the internal standard (Me_4Si). Spin-spin coupling constants were determined with an accuracy of 0.1 Hz. The solvent was DMSO-d_6. The 2D gs-HMQC, gs-HMBC, and gs-COSY procedures with pulse field gradients were used for signal assignment in the NMR spectra.

The reaction course was monitored by TLC on the DC-Fertigfolien ALUGRAM 60 UV254 plates (Macherey-Nagel). The compounds were purified on an IsoleraTM Prime preparative low-pressure liquid flash chromatograph (Biotage). Melting points were measured in capillaries on a Mel-temp II instrument and were not corrected. Elemental analysis was conducted on a Carlo Erba 1108 elemental analyzer at the Laboratory of Microanalysis of the A. N. Nesmeyanov Institute of Organoelement Compounds of the Russian Academy of Sciences. Mass spectra with electrospray ionization (ESI) were detected on Agilent 1100 (series LC/MSD) and Shimadzu LCMS-2020 mass spectrometers with direct sample injection into the ionization zone. High-resolution mass spectra were measured on a Shimadzu LCMS-9030 instrument (ESI).

Electronic absorption spectra were recorded on a Cary 300 two-channel spectrophotometer (Agilent). Fluorescence spectra were detected on a FluoroLog-3-221 spectrofluorimeter (Horiba Jobin Yvon). The observed fluorescence was detected at a right angle relative to the excitation beam. Fluorescence spectra were corrected with respect to the sensitivity of the measuring photoelectron multiplier.

Fluorescence quantum yields were determined in air-saturated acetonitrile solutions at room temperature. The quantum yields were calculated by the following equation[61]:

$$\varphi^{fl} = \varphi^{fl}_R \frac{S}{S_R} \cdot \frac{(1-10^{-A_R})n^2}{(1-10)^{-A} n_R^2}, \qquad (2)$$

where φ^{fl} and $\varphi^{fl}{}_R$ are the fluorescence yields of the analyzed solution and standard, respectively; A and A_R are the absorbances of the analyzed solution and standard, respectively; S and S_R are the surface areas under the curves of the fluorescence spectra of the analyzed solution and standard, respectively; and n and n_R are the refractive indices of the substance under study and standard compound, respectively Coumarin 481 in acetonitrile (quantum yield 0.08)[62] was used as the standard for the calculation of quantum yields.

The stability constants of the complexes of ligands **1** and **4** (L) with the mercury(II) cation were determined using spectrophotometric and spectrofluorimetric titration.[63,64] A solution of the ligand was prepared in an acetate buffer with the exactly known concentration (10^{-5} mol L^{-1}) in a quartz cell (l = 1 cm) by the dilution of a more concentrated solution of the ligand in DMSO

(the fraction of DMSO in the resulting solution was 1 vol.%), and the absorption (or fluorescence) spectrum was detected. Small portions (5—20 μL) of a solution of the metal salt in water (also with the known concentration) were added to the resulting solution. The absorption (fluorescence) spectrum was detected after every addition. Titration was accepted finished when the spectrum stopped changing upon the addition of the next portion of the titrant. The logarithm of the stability constant of the complex was calculated using the SPECFIT/32 program (Version 3.0.37). The possibility of formation of complexes according to the equilibria

$$L + Hg^{2+} \rightleftharpoons L \cdot Hg^{2+},$$

$$2\,L + Hg^{2+} \rightleftharpoons L_2 \cdot Hg^{2+}.$$

was taken into account in the calculation.

The experimental data on the dependence of the absorbance of the solution at wavelengths of 475 and 460 nm (in the case of the spectrophotometric titration of compounds **1** and **4**) or on the dependence of R (in the case of the spectrofluorimetric titration of compounds **1** and **4**) on the mercury(II) ion concentration in the solution are consistent with the theoretical calculation results only if taking into account the formation of 1 : 1 metal—ligand complexes (see Figs 1, *a*, *b*; 5, *a*, *b*, insets).

Quantum chemical calculations were performed using the MOPAC2016 software by the semiempirical PM6 method.[65] The iteration procedure was continued until the difference in energy of the molecule for two adjacent iterations became lower than 0.01 kcal mol^{-1}. The influence of the solvent nature was taken into account according to the COSMO (COnductorlike Screening Model) model implemented into MOPAC. It was accepted in the calculations that the solvent had the dielectric constant $\varepsilon = 80$ and such a refractive index (n) that $n^2 = 2$.

The efficiency of the RET process was calculated by the equation[57]

$$\Phi_{RET} = R_0^6/\left(R_0^6 + r^6\right), \qquad (3)$$

where r is the distance between the chromophoric fragments equal to 15 Å and determined with allowance for the data on the optimized geometry of compound **4** (see Fig. 3). The Förster critical radius (R_0) was determined by the equation[57]

$$R_0^6 = 8.79 \cdot 10^{-5}\left[\kappa^2 n^{-4} \varphi^{fl}_{CD,0} J(\lambda)\right], \qquad (4)$$

where κ^2 is the orientational factor determining the mutual arrangement of the dipole moments of the transitions of the energy donor and acceptor (accepted to be 2/3, which corresponds to the equiprobable orientation of the dipoles due to rotational diffusion of the molecular fragments before the energy transfer), $\varphi^{fl}_{CD,0}$ is the fluorescence quantum yield of CD in the absence of CA (for the quantum yield of compound **2**, see Table 1), n is the refractive index of the solvent, and $J(\lambda)$ is the overlapping integral of the surface area-corrected emission spectrum of CD with the absorption spectrum of CA ($nm^4\ L\ mol^{-1}\ cm^{-1}$). The $J(\lambda)$ values were calculated from the measured fluorescence spectrum of compound **2** ($I_{CD}(\lambda)$) and absorption spectra of compound **1** and complex $\mathbf{1} \cdot Hg^{2+}$ ($\varepsilon_{CA}(\lambda)$) by the equation[57]

$$J(\lambda) = \int_0^\infty I_{CD}(\lambda)\varepsilon_{CA}(\lambda)\lambda^4 d\lambda \Big/ \int_0^\infty I_{CD}(\lambda) d\lambda. \qquad (5)$$

The HEK293 embryonal cells of human kidney were grown in the DMEM/F12 medium (PanEko, Russia) with the addition of a 10% HyClone defined embryonal calf serum (GE Healthcare Life Sciences, USA) and glutamine (2 mmol L^{-1}) (PanEko, Russia). Reinoculations were made twice a week. For experiment, the cells being in the logarithmic growth were sowed on cover glasses in 24-well plates (2×105 cells in a well) and were grown at 37 °C for 24 h in the presence of CO_2 (5%).

A freshly prepared stock solution of compound **4** in DMSO with a concentration of 1 mmol L^{-1} was used for the studies. To study the intracellular penetration of the compound, the cells were incubated with compound **4** (1—20 μmol L^{-1}) for 0.5—3.0 h. To study the intracellular complex formation of compound **4** with Hg^{2+} ions, either the HEK293 cells were incubated with compound **4** (10 μmol L^{-1}) for 1.5 h and then washed with Hanks′ solution, $Hg(ClO_4)_2$ (10—50 μmol L^{-1}) was added, and the resulting mixture was incubated for 30—60 min; or the HEK293 cells were pre-incubated for 30—60 min with $Hg(ClO_4)_2$ (10—50 μmol L^{-1}), then washed with Hanks′ solution, and incubated with compound **4** for 0.5—2.0 h. When studying the colocalization of the compound with the Lyso Tracker Red (LR) fluorescent marker of lysosomes (Molecular Probes), the cells were incubated for 1 h with compound **4** (10 μmol L^{-1}) and LR (50 nmol L^{-1}).

Confocal fluorescent images were obtained on an LSM-710 confocal laser scanning microscope (Carl Zeiss AG, Oberkochen, Germany) using an α-Plan-Apochromat 100×/1.4 oil-immersion lens with a resolution of 1.5 μm in the direction of the optical axis of the microscope and of 0.3 μm in the perpendicular plane. When studying the intracellular penetration of compound **4** and its complex formation with Hg^{2+} ions, fluorescence was excited with a laser at a wavelength of 405 nm and detected in a spectral range of 420—730 nm. The intracellular fluorescence spectra of compound **4** were examined using the spectral mode of preparing confocal images: fluorescence was excited with a laser at a wavelength of 405 nm and detected in the spectral mode with an increment of 5 or 10 nm in a range of 420—730 nm.

When studying colocalization with lysosomes, fluorescence of compound **4** and LR was excited with lasers at

wavelengths of 405 and 543 nm and detected in ranges of 450—520 and 630—730 nm, respectively. The fluorescence spectra of compound **4** and LR are partially overlapped and, hence, the "unmixing" function was applied for the correction of the confocal images according to the equation

$$I_{\mathbf{4}} = \left(I_{450—520} - \beta I_{650—730}\right) / \left(1 - \alpha\beta\right), \quad (6)$$

$$I_{\mathrm{LR}} = \left(I_{650—730} - \alpha I_{450—520}\right) / \left(1 - \alpha\beta\right), \quad (7)$$

where I_{LR} and $I_{\mathbf{4}}$ are the real fluorescence intensities of LR and compound **4** in spectral ranges of 450—520 and 650—730 nm, respectively; $I_{450–520}$ and $I_{650–730}$ are the measured fluorescence intensities in spectral ranges of 450—520 and 650—730 nm, respectively; α is the fluorescence diffluencing coefficient of the compound in a spectral range of 650—730 nm; and β is the fluorescence diffluencing coefficient of LR in a spectral range of 450—520 nm. To determine the fluorescence diffluencing coefficients, the HEK293 cells were separately incubated only with compound **4** or with LR and measured under the same conditions.

(*E*)-6-(4-Methoxystyryl)-2-(prop-2-inyl)-1*H*-benzo[*d*,*e*]isoquinoline-1,3(2*H*)-dione (2). A mixture of anhydride **9** (215 mg, 0.652 mmol) and propargylamine (170 μL, 2.658 mmol) was refluxed for 10 h in 2-methoxyethane (10 mL) under an argon atmosphere. The reaction mixture was diluted with water, and the formed precipitate was filtered off, washed on the filter, dried in air, and recrystallized from methanol. Naphthalimide **2** as an orange powder was formed in a yield of 184 mg (77%), m.p. 225—226 °C. ^{1}H NMR (18 °C), δ: 3.64 (s, 1 H, C≡CH); 3.82 (s, 3 H, OCH_3); 4.78 (s, 2 H, CH_2); 7.02 (d, 2 H, C(13)H, C(15)H, *J* = 8.5 Hz); 7.58 (d, 1 H, C(10)H, *J* = 16.2 Hz); 7.82 (d, 2 H, C(12)H, C(16)H, *J* = 8.5 Hz); 7.86—7.94 (m, 1 H, C(6)H); 8.05 (d, 1 H, C(9)H, *J* = 16.2 Hz); 8.21 (d, 1 H, C(3)H, *J* = 8.1 Hz); 8.48 (d, 1 H, C(2)H, *J* = 8.1 Hz); 8.55 (d, 1 H, C(7)H, *J* = 7.1 Hz); 9.00 (d, 1 H, C(5)H, *J* = 8.9 Hz). ^{13}C NMR (100.60 MHz, 18 °C), δ: 29.55 (CH_2); 55.48 (C≡CH); 55.78 (OCH_3); 73.51 (C≡CH); 114.77 (C(13), C(15)); 120.30 (C(1)); 121.07 (C(9)); 122.44 (C(8)); 123.58 (C(3)); 127.44 (C(6)); 128.37 (C(8a)); 129.47 (C(4a)); 129.67 (C(12), C(16)); 130.77 (C(11)); 131.54 (C(7)); 131.91 (C(5)); 133.34 (C(2)); 135.77 (C(10)); 142.43 (C(4)); 160.43 (C(14)); 162.93 (C(8b)); 163.28 (C(8c)). MS (ESI, from a solution in $CHCl_3$): found *m*/*z* 368.18; calculated 368.13 $[M + H]^+$. Found (%): C, 77.08; H, 4.90; N, 3.45. $C_{24}H_{17}NO_3 \cdot 0.4\ CH_3OH$. Calculated (%): C, 77.08; H, 4.93; N, 3.68.

(*E*)-4-[4-(1,4-Dioxa-7,13-dithia-10-azacyclopentadecan-10-yl)styryl]-1-(3-azidopropyl)pyridinium bromide (3). A mixture of γ-picolinium salt **5** (0.10 g, 0.39 mmol), aldehyde **6** (0.15 g, 0.42 mmol), piperidine (16 μL), and *n*-butyl alcohol (5 mL) was refluxed in an oil bath for 4 h. Then the solvent was evaporated *in vacuo*, and the residue was chromatographed on a column with SiO_2 in a dichloromethane—methanol system of solvents using the gradient increasing the eluent polarity (from neat CH_2Cl_2 to a volume ratio of 4 : 1). Product **3** was isolated as a red powder (0.16 g, 69%). ^{1}H NMR (20 °C), δ: 2.16 (m, 2 H, C(26)H); 2.75 (m, 4 H, C(16)H, C(23)H); 2.83 (m, 4 H, C(17)H, C(22)H); 3.47 (t, 2 H, C(27)H, *J* = 6.3 Hz); 3.58 (s, 4 H, C(19)H, C(20)H); 3.67 (m, 4 H, C(18)H, C(21)H); 3.7 (m, 4 H, C(15)H, C(24)H); 4.48 (t, 2 H, C(25)H, *J* = 6.6 Hz); 6.72 (d, 2 H, C(11)H, C(13)H, *J* = 8.6 Hz); 7.17 (d, 1 H, C(7)H, *J* = 15.6 Hz); 7.59 (d, 2 H, C(10)H, C(14)H, *J* = 8.6 Hz); 7.93 (d, 1 H, C(8)H, *J* = 15.6 Hz); 8.08 (d, 2 H, C(3)H, C(5)H, *J* = 5.9 Hz); 8.78 (d, 2 H, C(2)H, C(6)H, *J* = 5.9 Hz). ^{13}C NMR (100.60 MHz, 20 °C), δ: 29.08 (C(17), C(22)); 29.51 (C(26)); 30.77 (C(16), C(23)); 47.62 (C(27)); 51.27 (C(18), C(21)); 56.88 (C(25)); 70.00 (C(19), C(20)); 72.95 (C(15), C(24)); 111.82 (C(11), C(13)); 117.27 (C(7)); 122.47 (C(3), C(5)); 122.71 (C(9)); 130.59 (C(10), C(14)); 142.09 (C(8)); 143.69 (C(2), C(6)); 149.02 (C(12)); 153.85 (C(4)). High-resolution (HR) MS (ESI, from a solution in MeCN): found *m*/*z* 514.2302; calculated for $[C_{26}H_{36}N_5O_2S_2]^+$ 514.2310.

4-[4-(1,4-Dioxa-7,13-dithia-10-azacyclopentadecan-10-yl)styryl]-1-[3-(4-{[6-(4-methoxystyryl)-1,3-dioxo-1*H*-benzo[*d*,*e*]isoquinolin-2(3*H*)-yl]methyl}-1*H*-1,2,3-triazol-1-yl)propyl]pyridinium bromide (4). A mixture of propargyl derivative **2** (48 mg, 0.131 mmol), azide **3** (77 mg, 0.130 mmol), diisopropylethylamine (45 μL, 0.259 mmol), copper(I) iodide (10 mg, 0.052 mmol), and DMF (3 mL) was held at 80 °C for 25 h under an argon atmosphere. The solvent was evaporated *in vacuo*, and the residue was chromatographed on a column with silica gel using a CH_2Cl_2—EtOH (50 : 1, vol/vol) mixture as eluent. The yield was 63 mg (50%), m.p. 243—244 °C. ^{1}H NMR (19 °C), δ: 2.69—2.78 (m, 4 H, C(16′)H, C(23′)H); 2.78—2.90 (m, 4 H, C(17′)H, C(22′)H); 3.54—3.60 (m, 4 H, C(19′)H, C(20′)H); 3.62—3.78 (m, 8 H, C(18′)H, C(21′)H, C(15′)H, C(24′)H); 3.82 (s, 3 H, OCH_3); 4.37—4.47 (m, 4 H, C(27′)H, C(25′)H); 5.30 (s, 2 H, C(17)H); 6.71 (d, 2 H, C(11′)H, C(13′)H, *J* = 8.6 Hz); 7.03 (d, 2 H, C(13)H, C(15)H, *J* = 8.2 Hz); 7.11 (d, 1 H, C(7′)H, *J* = 16.1 Hz); 7.52—7.64 (m, 3 H, C(10′)H, C(14′)H, C(10)H); 7.83 (d, 2 H, C(12)H, C(16)H, *J* = 8.2 Hz); 7.86—7.96 (m, 2 H, C(8′)H, C(6)H); 8.01 (d, 2 H, C(3′)H, C(5′)H, *J* = 6.1 Hz); 8.04—8.14 (m, 2 H, C(19)H, C(9)H); 8.23 (d, 1 H, C(3)H, *J* = 7.9 Hz); 8.49 (d, 1 H, C(2)H, *J* = 7.9 Hz); 8.56 (d, 1 H, C(7)H, *J* = 7.4 Hz); 8.69 (d, 2 H, C(2′)H, H(6′), *J* = 6.1 Hz); 9.03 (d, 1 H, C(5)H, *J* = 8.3 Hz). ^{13}C NMR (18 °C), δ: 29.47 (C(17′), C(22′)); 30.90 (C(26′)); 31.34 (C(16′), C(23′)); 46.55 (C(27′)); 51.82 (C(15′), C(24′)); 53.17 (C(25′)); 55.70 (OCH_3); 60.53 (C(17)); 70.47 (C(19′),

C(20′)); 72.33 (C(18′), C(21′)); 112.29 (C(11′), C(13′)); 114.78 (C(13), C(15)); 117.69 (C(7′)); 120.59 (C(1)); 121.20 (C(9)); 122.31 (C(8)); 122.89 (C(3′), C(5′)); 122.93 (C(9′)); 123.46 (C(3)); 123.49 (C(19)); 127.79 (C(6)); 128.72 (C(8a)); 129.32 (C(4a)); 129.71 (C(12), C(16)); 130.53 (C(11)); 130.57 (C(10′), C(14′)); 131.07 (C(7)); 131.33 (C(2)); 131.90 (C(5)); 135.66 (C(10)); 142.26 (C(8′)); 142.35 (C(4)); 143.60 (C(18)); 144.07 (C(2′), C(6′)); 149.34 (C(12′)); 154.54 (C(4′)); 160.48 (C(14)); 163.38 (C(8b)); 163.81 (C(8c)). HR MS (ESI, from a solution in MeCN): found *m/z* 881.3522; calculated for $[C_{50}H_{53}N_6O_5S_2]^+$ 881.3519.

(*E*)-6-(4-Methoxystyryl)benzo[*d*,*e*]isochromene-1,3-dione (9). A solution of 4-bromonaphthalic anhydride (**8**) (70 mg, 0.253 mmol), $Pd(OAc)_2$ (3 mg, 0.003 mmol), tris(*o*-tolyl)phosphine (5 mg, 0.016 mmol), triethylamine (420 μL), and styrene **7** (50 μL, 0.373 mmol) in anhydrous DMF (5 mL) was stirred at 105 °C for 8 h under an argon atmosphere. The reaction mixture was diluted with water, and the precipitate was filtered off, washed with water and ethanol, and dried. Product **9** was synthesized in a yield of 59 mg (71%), m.p. 184—185 °C. ^{1}H NMR (18 °C), δ: 3.82 (s, 3 H, OCH_3); 7.03 (d, 2 H, C(13)H, C(15)H, J = 8.6 Hz); 7.63 (d, 1 H, C(10)H, J = 16.1 Hz); 7.84 (d, 2 H, C(12)H, C(16)H, J = 8.6 Hz); 7.90—7.97 (m, 1 H, C(6)H); 8.09 (d, 1 H, C(9)H, J = 16.1 Hz); 8.27 (d, 1 H, C(3)H, J = 7.8 Hz); 8.48 (d, 1 H, C(2)H, J = 7.8 Hz); 8.55 (d, 1 H, C(7)H, J = 7.4 Hz); 9.09 (d, 1 H, C(5)H, J = 8.4 Hz). ^{13}C NMR (18 °C), δ: 55.39 (OCH_3); 114.27 (C(13), C(15)); 116.19 (C(1)); 119.23 (C(8)); 120.22 (C(9)); 123.16 (C(3)); 127.15 (C(6)); 129.01 (C(4a)); 129.30 (C(12), C(16)); 129.78 (C(11)); 130.65 (C(4a)); 132.06 (C(5)); 132.33 (C(2)); 132.54 (C(7)); 135.83 (C(10)); 142.73 (C(4)); 160.07 (C(14)); 160.64 (C(8b)); 161.04 (C(8c)). MS (ESI, from a solution in $CHCl_3$): found *m/z* 331.18; calculated 331.10 $[M + H]^+$. Found (%): C, 72.41; H, 4.59. $C_{21}H_{14}O_4 \cdot H_2O$. Calculated (%): C, 72.41; H, 4.63.

Acknowledgments

The spectral characteristics of the synthesized compounds were studied with the support of the Ministry of Science and Higher Education of the Russian Federation using the scientific equipment of the Center for Collective Use of Molecule Structure Investigation at the A. N. Nesmeyanov Institute of Organoelement Compounds of the Russian Academy of Sciences.

Funding

This work was financially supported by the Russian Science Foundation (Project No. 20-73-10186-P).

Animal Testing and Ethics

No human or animal subjects were used in this research.

Conflict of Interest

The authors declare no competing interests.

References

1. V. F. Traven, D. A. Cheptsov, *Russ. Chem. Rev.*, 2020, **89**, 713—749; DOI: 10.1070/RCR4909.
2. F. Wang, K. Wang, Q. Kong, J. Wang, D. Xi, B. Gu, S. Lu, T. Wei, X. Chen, *Coord. Chem. Rev.*, 2021, **429**, Art. No. 213636; DOI: 10.1016/j.ccr.2020.213636.
3. G. Sivaraman, M. Iniya, T. Anand, N. G. Kotla, O. Sunnapu, S. Singaravadivel, A. Gulyani, D. Chellappa, *Coord. Chem. Rev.*, 2018, **357**, 50—104; DOI: 10.1016/j.ccr.2017.11.020.
4. M. Formica, V. Fusi, L. Giorgi, M. Micheloni, *Coord. Chem. Rev.*, 2012, **256**, 170—192; DOI: 10.1016/j.ccr.2011.09.010.
5. L. S. Atabekyan, V. G. Avakyan, N. A. Alexandrova, M. V. Fomina, S. P. Gromov, *Russ. Chem. Bull.*, 2023, **72**, 877—894; DOI: 10.1007/s11172-023-3851-6.
6. M. A. Pavlova, P. A. Panchenko, M. N. Vlasova, O. A. Fedorova, *Russ. Chem. Bull.*, 2023, **72**, 2154—2161; DOI: 10.1007/s11172-023-4011-y.
7. L. Deng, Y. Li, X. Yan, J. Xiao, C. Ma, J. Zheng, S. Liu, R. Yang, *Anal. Chem.*, 2015, **87**, 2452—2458; DOI: 10.1021/ac504538v.
8. A. F. Castoldi, C. Johansson, N. Onishchenko, T. Coccini, E. Roda, M. Vahter, S. Ceccatelli, L. Manzo, *Regul. Toxicol. Pharmacol.*, 2008, **51**, 215—229; DOI: 10.1016/j.yrtph.2008.03.005.
9. H. H. Harris, I. J. Pickering, G. N. George, *Science*, 2003, **301**, 1203; DOI: 10.1126/science.1085941.
10. M. Harada, B. R. Von, *J. Appl. Toxicol.*, 1995, **15**, 483; DOI: 10.1002/jat.2550150610.
11. K. M. Rice, E. M. Walker, M. Wu, C. Gillette, E. R. Blough, *J. Prev. Med. Public Health*, 2014, **47**, 74—83; DOI: 10.3961/jpmph.2014.47.2.74.
12. B. Fernandes Azevedo, L. Barros Furieri, F. M. Peçanha, G. A. Wiggers, P. Frizera Vassallo, M. Ronacher Simões, J. Fiorim, P. Rossi de Batista, M. Fioresi, L. Rossoni, I. Stefanon, M. J. Alonso, M. Salaices, D. Valentim Vassallo, *J. Biomed. Biotechnol.*, 2012, **2012**, 949048; DOI: 10.1155/2012/949048.
13. H. Shuai, C. Xiang, L. Qian, F. Bin, L. Xiaohui, D. Jipeng, Z. Chang, L. Jiahui, Z. Wenbin, *Dyes Pigm.*, 2021, **187**, Art. No. 109125; DOI: 10.1016/j.dyepig.2020.109125.

14. V. Bhardwaj, V. M. Nurchi, S. K. Sahoo, *Pharmaceuticals*, 2021, **14**, Art. No. 123; DOI: 10.3390/ph14020123.
15. S. P. Kollur, C. Shivamallu, S. K. Prasad, R. Veerapur, S. S. Patil, C. A. Cull, J. F. Coetzee, R. G. Amachawadi, *Separations*, 2021, **8**, Art. No. 192; DOI: 10.3390/separations8100192.
16. A. P. Demchenko, *Lab. Chip.*, 2005, **5**, 1210—1223; DOI: 10.1039/B507447A.
17. A. P. Demchenko, *J. Fluoresc.*, 2010, **20**, 1099—1128; DOI: 10.1007/s10895-010-0644-y.
18. R. Gui, H. Jin, X. Bu, Y. Fu, Z. Wang, Q. Liu, *Coord. Chem. Rev.*, 2019, **383**, 82—103; DOI: 10.1016/j.ccr.2019.01.004.
19. A. P. Demchenko, *Methods Appl. Fluoresc.*, 2023, **11**, Art. No. 033001; DOI: 10.1088/2050-6120/acc715.
20. A. P. de Silva,T. S. Moody, G. D. Wrighta, *Analyst.*, 2009, **134**, 2385—2393; DOI: 10.1039/B912527M.
21. B. Valeur, M. N. Berberan-Santos, *Mol. Fluor. Principles and Applications*, 2012, **9**, 569; DOI: 10.1002/9783527650002.
22. A. Kim, S. Kim, C. Kim, *J. Chem. Sci.*, 2020, **132**, Art. No. 82; DOI: 10.1007/s12039-020-01789-y.
23. B. Shi, P. Zhang, T. Wei, H. Yao, Q. Lin, J. Liu, Y. Zhang, *Tetrahedron*, 2013, **69**, 7981—7987; DOI: 10.1016/j.tet.2013.07.007.
24. B. K. Momidi, V. Teruri, D. R. Trivedi, *Inorg. Chem. Commun.*, 2016, **74**, 1—5; DOI: 10.1016/j.inoche.2016.10.017.
25. H. Dai, F. Liu, Q. Gao, T. Fu, X. Kou, *Luminescence*, 2011, **26**, 523—530; DOI: 10.1002/bio.1264.
26. X.-L. Ni, Y. Wu, C. Redshaw, T. Yamato, *Dalton Trans.*, 2014, **43**, 12633—12638; DOI: 10.1039/c4dt01310g.
27. A. Barba-Bon, A. M. Costero, S. Gil, M. Parra, J. Soto, R. Martínez-Máñez, F. Sancenón, *Chem. Commun.*, 2012, **48**, 3000—3002; DOI: 10.1039/c2cc17184h.
28. B. T. Huy, D. T. Thangadurai, M. Sharipov, N. N. Nghia, N. V. Cuong, Y.-I. Lee, *Microchem. J.*, 2022, **179**, Art. No. 107511; DOI: 10.1016/j.microc.2022.107511.
29. D. S. Kopchuk, A. M. Prokhorov, P. A. Slepukhin, D. N. Kozhevnikov, *Tetrahedron Lett.*, 2012, **53**, 6265—6268; DOI: 10.1016/j.tetlet.2012.09.027.
30. K. Hanaoka, Y. Muramatsu, Y. Urano, T. Terai, T. Nagano, *Chem. Eur. J.*, 2010, **16**, 568—572; DOI: 10.1002/chem.200901591.
31. S. Erdemir, M. Oguz, S. Malkondu, *Anal. Chim. Acta*, 2022, **1192**, Art. No. 339353; DOI: 10.1016/j.aca.2021.339353.
32. P. A. Panchenko, Y. V. Fedorov, O. A. Fedorova, G. Jonusauskas, *Dyes Pigm.*, 2013, **98**, 347—357; DOI: 10.1016/j.dyepig.2013.03.008.
33. J. Fan, M. Hu, P. Zhan, X. Peng, *Chem. Soc. Rev.*, 2013, **42**, 29—43; DOI: 10.1039/c2cs35273g.
34. S.-H. Park, N. Kwon, J.-H. Lee, J. Yoon, I. Shin, *Chem. Soc. Rev.*, 2020, **49**, 143—179; DOI: 10.1039/c9cs00243j.
35. D. Cao, L. Zhu, Z. Liu, W. Lin, *J. Photochem. Photobiol. C*, 2020, **44**, Art. No. 100371; DOI: 10.1016/j.jphotochemrev.2020.100371.
36. W. Zhao, X. Liu, H. Lv, H. Fu, Y. Yang, Z. Huang, A. Han, *Tetrahedron Lett.*, 2015, **56**, 4293—4298; DOI: 10.1016/j.tetlet.2015.05.045.
37. R. Zhang, F. Yan, Y. Huang, D. Kong, Q. Ye, J. Xu, L. Chen, *RSC Adv.*, 2016, **6**, 50732—50760; DOI: 10.1039/c6ra06956h.
38. X. Zhang, Y. Xiao, X. Qian, *Angew. Chem., Int. Ed.*, 2008, **47**, 8025—8029; DOI: 10.1002/ANIE.200803246.
39. G. Singh, S. I. Reja, V. Bhalla, D. Kaur, P. Kaur, S. Arora, M. Kumar, *Sens. Actuators B*, 2017, **249**, 311—320; DOI: 10.1016/J.SNB.2017.04.074.
40. Y. Li, S. Qi, C. Xia, Y. Xu, G. Duan, Y. Ge, *Anal. Chim. Acta*, 2019, **1077**, 243—248; DOI: 10.1016/J.ACA.2019.05.043.
41. P. A. Panchenko, A. V. Efremenko, A. S. Polyakova, A. V. Feofanov, M. A. Ustimova, Y. V. Fedorov, O. A. Fedorova, *Biosensors*, 2022, **12**, Art. No. 770; DOI: 10.3390/bios12090770.
42. P. A. Panchenko, A. V. Efremenko, A. V. Feofanov, M. A. Ustimova, Y. V. Fedorov, O. A. Fedorova, *Sensors*, 2021, **21**, Art. No. 470; DOI: 10.3390/s21020470.
43. P. Gopikrishna, N. Meher, P. K. Iyer, *ACS Appl. Mater. Interfaces*, 2018, **10**, 12081—12111; DOI: 10.1021/acsami.7b14473.
44. W. Nie, L. Hu, *Chemistry Select.*, 2024, **9**, Art. No. e202303779; DOI: 10.1002/slct.202303779.
45. O. A. Fedorova, A. N. Sergeeva, P. A. Panchenko, Yu. V. Fedorov, F. G. Erko, J. Berthet, S. Delbaere, *J. Photochem. Photobiol. A*, 2015, **303**, 28—35; DOI: 10.1016/j.jphotochem.2015.02.004.
46. P. A. Panchenko, A. N. Sergeeva, O. A. Fedorova, Yu. V. Fedorov, R. I. Reshetnikov, A. E. Schelkunova, M. A. Grin, A. F. Mironov, G. Jonusauskas, *J. Photochem. Photobiol. B*, 2014, **133**, 140—144; DOI: 10.1016/j.jphotobiol.2014.03.008.
47. S. O.Aderinto, S. Imhanria, *Chem. Pap.*, 2018, **72**, 1823—1851; DOI: 10.1007/s11696-018-0411-0.
48. P. A. Panchenko, P. A. Ignatov, M. A. Zakharko, Yu. V. Fedorov, O. A. Fedorova, *Mendeleev Commun.*, 2020, **30**, 55—58; DOI: 10.1016/j.mencom.2020.01.018.
49. H.-Q. Dong, T.-B. Wei, X.-Q. Ma, Q.-Y. Yang, Y.-F. Zhang, Y.-J. Sun, B.-B. Shi, H. Yao, Y.-M. Zhang, Q. Lin, *J. Mater. Chem. C*, 2020, **8**, 13501—13529; DOI: 10.1039/d0tc03681a.
50. A. S. Oshchepkov, M. S. Oshchepkov, M. V. Oshchepkova, A. Al-Hamry, O. Kanoun, E. A. Kataev, *Adv. Opt. Mater.*, 2021. **9**, Art. No. 2001913; DOI: 10.1002/adom.202001913.

51. N. Jain, N. Kaur, *Coord. Chem. Rev.*, 2022, **459**, Art. No. 214454; DOI: 10.1016/j.ccr.2022.214454.
52. G. Kaur, I. Singh, N. Tandon, R. Tandon, A. Bhat, *Chemistry Select.*, 2023, **8**, Art. No. e202301661; DOI: 10.1002/slct.202301661.
53. P. A. Panchenko, Yu. V. Fedorov, O. A. Fedorova, *Russ. Chem. Rev.*, 2014, **83**, 155—182; DOI: 10.1070/RC2014v083n02ABEH004380.
54. H. Lv, G. Yuan, G. Zhang, Z. Ren, H. He, Q. Sun, X. Zhang, S. Wang, *Dyes and Pigments*, 2020, **172**, 107658; DOI: 10.1016/j.dyepig.2019.107658.
55. P. A. Panchenko, Yu. V. Fedorov, O. A. Fedorova, *J. Photochem. Photobiol. A.*, 2018, **364**, 124—129; DOI: 10.1016/j.jphotochem.2018.06.003.
56. P. A. Panchenko, A. S. Polyakova, Yu. V. Fedorov, O. A. Fedorova, *Mendeleev Commun.*, 2019, **29**, 155—157; DOI: 10.1016/j.mencom.2019.03.012.
57. J. R. Lakowicz, *Principles of Fluorescence Spectroscopy*, Springer Science & Business Media, New York, 2006, 954 pp.
58. H.-P. Loock, P. D. Wentzell, *Sens. Actuators B*, 2012, **173**, 157—163; DOI: 10.1016/j.snb.2012.06.071.
59. G.-H. Chen, W.-Y. Chen, Y.-C. Yen, C.-W. Wang, H.-T. Chang, C.-F. Chen, *Anal. Chem.*, 2014, **86**, 6843—6849; DOI: 10.1021/ac5008688.
60. S. Ohkuma, B. Poole, *Proc. Natl. Acad. Sci. USA*, 1978, **75**, 3327—3331; DOI: 10.1073/pnas.75.7.3327.
61. C. L. Renschler, L. A. Harrah, *Anal. Chem.*, 1983, **55**, 798—800; DOI: 10.1021/ac00255a050.
62. S. Nad, M. Kumbhakar, H. Pal, *J. Phys. Chem. A*, 2003, **107**, 4808—4816; DOI: 10.1021/jp021543t.
63. K. A. Connors, *Binding Constants: the Measurement of Molecular Complex Stability*, John Wiley & Sons, New York, 1987, **91**, 1398; DOI: 10.1002/bbpc.19870911223.
64. M. T. Beck, I. Nagypál, *Chemistry of Complex Equilibria*, John Wiley & Sons, New York, 1990.
65. J. Stewart, *J. Mol. Modeling*, 2007, **13**, 1173; DOI: 10.1007/s00894-007-0233-4.

Received March 13, 2024;
in revised form April 17, 2024;
accepted April 27, 2024